Complex band structure of two-dimensional thermal wave crystals

C. A. Romero-Ramos, J. Manzanares-Martinez*, and D. Soto-Puebla

Departamento de Investigación en Física, Universidad de Sonora, Hermosillo, Sonora 83000, México.

**e-mail: jesus.manzanares@unison.mx*

B. Manzanares-Martinez

Departamento de Física, Universidad de Sonora, Hermosillo, Sonora 83000, México.

Received 26 June 2024; accepted 3 July 2024

We investigate the complex band structure of temperature oscillations in a two-dimensional thermal wave crystal. We use the Cattaneo-Vernotte heat model to describe the thermal properties. We apply the plane wave method to calculate the complex band structure of a square lattice composed of an infinite array of square bars. We find that a complete band gap exists across the first Brillouin zone, where temperature oscillations are forbidden. This has potential applications in thermal management, thermal cloaking, and other areas.

Keywords: Complex band; Cattaneo-Vernotte.

DOI: https://doi.org/10.31349/RevMexFis.70.061603

1. Introduction

Fourier's law is the foundation of classical heat conduction analysis. It states that the heat flux is proportional to the negative gradient of temperature. When combined with the law of energy conservation this gives rise to a parabolic-type heat conduction equation. The problem with this equation is that its solutions assume an infinite speed for heat transmission [1]. This is incompatible with the observed finite speed of heat propagation in many materials, such as ultra-low-temperature systems [2], biological tissues [3], and nanomaterials [4]. To address this issue, models with non-Fourier heat conduction equations have been developed. These non-Fourier models take into account the finite speed of heat propagation, and they can be used to accurately model heat transfer in a wide range of materials [5].

In 1958 the first non-Fourier heat model was developed independently by Cattaneo [6] and Vernotte [7] introducing a time delay between the heat flux and the temperature gradient. This modification known as the Cattaneo-Vernotte (CV) model, allows for a finite speed of heat propagation. The CV model is consistent with experimental results in a variety of materials [8]. This makes it a valuable tool for modeling heat transfer in non-Fourier materials where the finite speed of heat propagation is important.

The CV model is the simplest method to analyze non-Fourier heat propagation. However, it is a relatively crude model because it incorporates all the microscopic effects of heat conduction into a single time delay parameter. To describe the physical process more precisely, other non-Fourier heat conduction models have been developed, such as the dual-phase-lag model [9] and the three-phase-dual model [10]. Recently, A. I. Zhmakin reported a review of non-Fourier heat conduction models [5].

The manipulation of waves is a key issue for the control of energy via interference phenomena. In the case of a time-harmonic source of heat, there exist wave-like solutions for the CV model where the interference of temperature oscillations is possible. Considering the possibility of thermal waves in periodic media, in 2018, A. L. Chen *et al* reported the band structure for thermal wave oscillations in a one-dimensional Thermal Wave Crystal (TWC) [11]. TWCs are periodic arrays of two materials where thermal oscillations and interference phenomena of waves can exist in a composite medium. The periodicity of a TWC is described by the position-dependent parameters of density $\rho(\mathbf{x})$, specific heat $c(\mathbf{x})$, thermal conductivity $\kappa(\mathbf{x})$, and time delay $\tau(\mathbf{x})$.

In this paper, we investigate the complex band structure of two-dimensional periodic structures made of materials that follow the CV model. We apply the plane-wave method (PWM) to calculate the complex band structure. Our results show that it is possible to obtain a complete band gap in the First Brillouin Zone. The complex band structure is determined by considering an eigenvalue-problem with the wave vector as the eigenvalue, $\mathbf{k}(\omega)$.

Our inspiration for determining the complex band structure comes from the study of photonic crystals (PCs) [12]. PCs are periodic structures that exhibit band gaps for electromagnetic waves. Most PCs have a real and frequency-independent dielectric function. For this type of PCs, the PWM has been widely used to calculate the band structure by solving an eigenvalue problem for the frequency at a fixed wave vector, $\omega(\mathbf{k})$.

In the field of PCs, some researchers have become interested in structures with frequency-dependent, dispersive, or dissipative material components [13,14]. The existence of frequency-dependent components in a PC introduces difficulty in the calculation because it is no longer possible to

obtain a canonical eigenvalue problem with the frequency as an eigenvalue. The problem must be modified to determine the wave vector at a fixed frequency, $\mathbf{k}(\omega)$.

The proposal to control heat conduction via interference phenomena in periodic structures has recently attracted widespread attention, both theoretically and experimentally [15]. The absence of temperature oscillations in a periodic lattice can lead to unusual physical phenomena for thermal conduction [16]. The idea is to create thermal metamaterials that can control the flux of heat, similarly to how light is controlled by PCs. For example, a defect state in a periodic structure can be locked in an excited state if its energy falls within the band gap. The possible applications of TWC include heat waveguides [17], thermal isolators [18-20], thermal diodes [21]. and thermal cloaking [22].

Of particular interest is the prospect of achieving a complete band gap, which is defined as a stop band in which thermal vibrations are prohibited for all Bloch vectors. There are many important motivations for pursuing this study. For instance, recent studies have shown that it is possible to control the flow of heat to design architected thermal devices, such as thermal camouflage and concentrators [23].

The band structure of TWCs has been calculated for only a few cases to date. For the case of one-dimensional TWCs, the band structure has been calculated using the Transfer Matrix Method (TMM) for two different models: the CV model [11,24-26] and the dual-phase-lag (DPL) model [27]. Recently, we have applied the PWM for the case of CV model [28].

For the case of two-dimensional TWCs, the band structure has been calculated for the CV and DPL models by solving an eigenvalue problem using COMSOL Multiphysics [29]. Additionally, an attempt has been made to utilize PWM; however, it has not been appropriately implemented in a wave equation that captures the position-dependent material parameters [30].

In this paper, we perform the band structure calculation of 2D TWC using the PWM. The theoretical details are described as follows. In Sec. 2, we present the deduction of the wave equation in the frequency domain. In Sec. 3 we apply the PWM to the wave equation. Section 4 presents our results and finally in Sec. 5 we have our conclusions.

2. The wave equation in the frequency-domain

The CV heat conduction model proposes a modification of Fourier's law by introducing a time delay into the heat flux vector, in the form [6,7]

$$\mathbf{q}[\mathbf{x}, t+\tau(\mathbf{x})] = -\kappa(\mathbf{x})\nabla T(\mathbf{x}, t), \tag{1}$$

where $T(\mathbf{x}, t)$, $\mathbf{q}(\mathbf{x}, t)$, $\kappa(\mathbf{x})$ and $\tau(\mathbf{x})$ are the position-dependent temperature, flux vector, thermal conductivity, and time delay respectively. We expand the left-hand side of Eq. (1) using the Taylor series, retaining only the first two terms to have

$$\mathbf{q}(\mathbf{x}, t) + \tau(\mathbf{x})\frac{\partial}{\partial t}\mathbf{q}(\mathbf{x}, t) = -\kappa(\mathbf{x})\nabla T(\mathbf{x}, t). \tag{2}$$

The equation of energy conservation in the absence of internal energy sources is given by

$$\nabla \cdot \mathbf{q}(\mathbf{x}, t) = -\rho(\mathbf{x})c(\mathbf{x})\frac{\partial}{\partial t}T(\mathbf{x}, t), \tag{3}$$

where $\rho(\mathbf{x})$ and $c(\mathbf{x})$ are the position-dependent density and specific heat, respectively.

In this work, we investigate thermal wave propagation in a 2D periodic lattice, where $x-y$ is the plane of periodicity. The medium along the z-axis is homogeneous, and the propagation of the wave vector $\mathbf{k}$ is parallel to the periodicity plane. We analyze a periodic structure that has a square unit cell of length D, which is illustrated in Fig. 1a). The dark-gray square of length d corresponds to material a and is surrounded by another light-gray medium, which corresponds to material b. We consider a structure where we have the following periodic parameters: density $\rho(\mathbf{x}) = \rho(\mathbf{x}+\mathbf{R})$, specific heat $c(\mathbf{x}) = c(\mathbf{x}+\mathbf{R})$, thermal conductivity $\kappa(\mathbf{x}) = \kappa(\mathbf{x}+\mathbf{R})$, and time delay $\tau(\mathbf{x}) = \tau(\mathbf{x}+\mathbf{R})$, where $\mathbf{R} = D(n_x\hat{i} + n_y\hat{j})$ is a lattice vector in the $x-y$ plane defined by the integers n_x and n_y. We seek to find the band structure for an infinite array of parallel rods of square section with their axes cutting the $x-y$ plane in the $\mathbf{R}$ sites of a square lattice, as we illustrate in Fig. 1b).

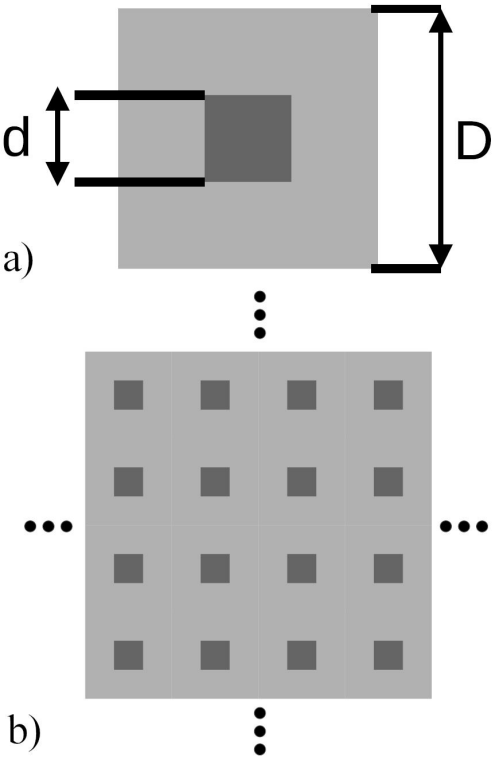

FIGURE 1. a) Square unit cell of side D. The square cylinder at the center has a side d. The dark gray zone at the center corresponds to material a and the surrounding area corresponds to material b. b) Infinite lattice constructed by the repetition of the unit cell.

The position-dependence of the material parameters in the unit cell are given by the following equations, for the density

$$\rho(\mathbf{x}) = \rho_b + (\rho_a - \rho_b)\,\theta\left(\frac{D}{2} - |x|\right)\left(\frac{D}{2} - |y|\right), \quad (4)$$

heat capacity

$$c(\mathbf{x}) = c_b + (c_a - c_b)\,\theta\left(\frac{D}{2} - |x|\right)\left(\frac{D}{2} - |y|\right), \quad (5)$$

thermal conductivity

$$\kappa(\mathbf{x}) = \kappa_b + (\kappa_a - \kappa_b)\,\theta\left(\frac{D}{2} - |x|\right)\left(\frac{D}{2} - |y|\right), \quad (6)$$

and time delay

$$\tau(\mathbf{x}) = \tau_b + (\tau_a - \tau_b)\,\theta\left(\frac{D}{2} - |x|\right)\left(\frac{D}{2} - |y|\right), \quad (7)$$

respectively. In Eqs. (4)-(7) the values of ρ_a, c_a, κ_a and τ_a correspond to the values of material a and, in the same manner ρ_b, c_b, κ_b and τ_b correspond to the values of material b. The Heaviside function is defined by

$$\theta(\alpha) = \begin{cases} 1, & \text{if } \alpha \geq 0 \\ 0, & \text{if } \alpha < 0 \end{cases}. \quad (8)$$

Considering the case of harmonic thermal waves, the Fourier transform allows switching from the time domain into the frequency domain. The Fourier Transforms for the temperature and heat flux are [31]

$$T(\mathbf{x}, t) = \frac{1}{\sqrt{2\pi}} \int_{-\infty}^{\infty} T(\mathbf{x}, \omega) e^{-i\omega t} d\omega, \quad (9)$$

and

$$\mathbf{q}(\mathbf{x}, t) = \frac{1}{\sqrt{2\pi}} \int_{-\infty}^{\infty} \mathbf{q}(\mathbf{x}, \omega) e^{-i\omega t} d\omega. \quad (10)$$

In the frequency domain, Eqs. (2) and (3) can be written as

$$\mathbf{q}(\mathbf{x}, \omega)[1 - i\omega\tau(\mathbf{x})] = -\kappa(\mathbf{x})\nabla T(\mathbf{x}, \omega), \quad (11)$$

and

$$\nabla \cdot \mathbf{q}(\mathbf{x}, \omega) = i\omega\rho(\mathbf{x})c(\mathbf{x})T(\mathbf{x}, \omega). \quad (12)$$

Combining Eqs. (11) and (12) we obtain

$$\nabla \cdot \alpha(\mathbf{x})\nabla T(\mathbf{x}, \omega) = i\omega\beta(\mathbf{x})T(\mathbf{x}, \omega), \quad (13)$$

where we have defined

$$\alpha(\mathbf{x}) = \frac{\kappa(\mathbf{x})}{i\omega\tau(\mathbf{x}) - 1}, \quad (14)$$

and

$$\beta(\mathbf{x}) = \rho(\mathbf{x})c(\mathbf{x}). \quad (15)$$

The functions $\alpha(\mathbf{x})$ and $\beta(\mathbf{x})$ are periodic position-dependent variables defined by

$$\alpha(\mathbf{x}) = \alpha_b + (\alpha_a - \alpha_b)\,\theta\left(\frac{D}{2} - |x|\right)\left(\frac{D}{2} - |y|\right), \quad (16)$$

and

$$\beta(\mathbf{x}) = \beta_b + (\beta_a - \beta_b)\,\theta\left(\frac{D}{2} - |x|\right)\left(\frac{D}{2} - |y|\right), \quad (17)$$

where we have introduced the following variables

$$\alpha_a = \frac{\kappa_a}{i\omega\tau_a - 1}, \quad (18)$$

$$\alpha_b = \frac{\kappa_b}{i\omega\tau_b - 1}, \quad (19)$$

$$\beta_a = \rho_a c_a, \quad (20)$$

and

$$\beta_b = \rho_b c_b. \quad (21)$$

3. The eigenvalue equation for the complex wave vector

In this section, we investigate the utilization of the PWM technique in the analysis of complex band structures. Notably, Zheng-Yang Li *et al* recently employed the PWM method to study two-dimensional structures [30]. It is noteworthy that in their work, the PWM technique was employed to examine a wave equation that specifically characterizes a homogeneous medium. However, for the PWM approach to be effectively applied, it is crucial to have a wave equation that allows for the definition of position-dependent material parameters within the unit cell. Our derived Eq. (13) in Sec. 2 serves as an illustrative example of such an equation, highlighting the significance of this capability.

Since the medium is periodic, the material parameters are periodic and can be expanded as a Fourier series in the form

$$\alpha(\mathbf{x}) = \sum_{\mathbf{G}} \alpha_{\mathbf{G}} e^{i\mathbf{G}\cdot\mathbf{x}} \quad (22)$$

and

$$\beta(\mathbf{x}) = \sum_{\mathbf{G}} \beta_{\mathbf{G}} e^{i\mathbf{G}\cdot\mathbf{x}}, \quad (23)$$

where $\alpha_{\mathbf{G}}$ and $\beta_{\mathbf{G}}$ are Fourier coefficients. The reciprocal lattice vectors are defined as

$$\mathbf{G} = G_x\hat{i} + G_y\hat{j} = \frac{2\pi}{D}(m_x\hat{i} + m_y\hat{j}), \quad (24)$$

where m_x and m_y are integer numbers.

The Fourier coefficients are obtained by integrating Eqs. (22) and (23) in the form

$$\alpha_{\mathbf{G}} = \frac{1}{D^2}\int_{-D/2}^{D/2}\int_{-D/2}^{D/2}\alpha(\mathbf{x})\exp(-i\mathbf{G}\cdot\mathbf{x})dxdy, \quad (25)$$

and

$$\beta_{\mathbf{G}} = \frac{1}{D^2}\int_{-D/2}^{D/2}\int_{-D/2}^{D/2}\beta(\mathbf{x})\exp(-i\mathbf{G}\cdot\mathbf{x})dxdy. \quad (26)$$

After integrating Eqs. (25) and (26) we obtain

$$\alpha_{\mathbf{G}} = [\alpha_b + f(\alpha_a-\alpha_b)]\,\delta_{\mathbf{G},0} + f(\alpha_a-\alpha_b) \times \frac{\sin(G_x(d/2))}{G_x(d/2)}\frac{\sin(G_y(d/2))}{G_y(d/2)}(1-\delta_{\mathbf{G},0}), \quad (27)$$

and

$$\beta_{\mathbf{G}} = [\beta_b + f(\beta_a-\beta_b)]\,\delta_{\mathbf{G},0} + f(\beta_a-\beta_b) \times \frac{\sin(G_x(d/2))}{G_x(d/2)}\frac{\sin(G_y(d/2))}{G_y(d/2)}(1-\delta_{\mathbf{G},0}), \quad (28)$$

where the filling fraction f is

$$f = \left(\frac{d}{D}\right)^2. \quad (29)$$

The temperature satisfies the Bloch Theorem and can be expanded in terms of plane waves in the form

$$T(\mathbf{x},\omega) = \sum_{\mathbf{G}} T_{\mathbf{G}} e^{i(\mathbf{k}+\mathbf{G})\cdot\mathbf{x}}, \quad (30)$$

where $\mathbf{k}$ is a wave vector in the first Brillouin zone. Substitution of Eqs. (22), (23) and (30) in Eq. (13) yields

$$\sum_{\mathbf{G}'}\left[\alpha_{\mathbf{G}-\mathbf{G}'}(\mathbf{k}+\mathbf{G})\cdot(\mathbf{k}+\mathbf{G}') + i\omega\beta_{\mathbf{G}-\mathbf{G}'}\right]T_{\mathbf{G}'} = 0. \quad (31)$$

To solve this equation, we write an eigenvalue problem for the directions of high symmetry defined by the directions $\mathbf{\Gamma}\rightarrow\mathbf{X}$, $\mathbf{X}\rightarrow\mathbf{M}$ and $\mathbf{M}\rightarrow\mathbf{\Gamma}$, where $\mathbf{\Gamma} = (0,0)$, $\mathbf{X} = [(2\pi)/D](1/2,0)$ and $\mathbf{M} = [(2\pi)/D](1/2,1/2)$.

3.1. $\mathbf{\Gamma}\rightarrow\mathbf{X}$ direction

In this direction, the wave vector is only in the x-direction, $\mathbf{k} = (k_x, 0)$. In this case, it is possible to write the Eq. (31) as

$$\sum_{\mathbf{G}'}\left[k_x^2 A_{\mathbf{G}-\mathbf{G}'} + k_x B_{\mathbf{G}-\mathbf{G}'} + C_{\mathbf{G}-\mathbf{G}'}\right]T_{\mathbf{G}'} = 0, \quad (32)$$

where we have introduced

$$A_{\mathbf{G}-\mathbf{G}'} = \alpha_{\mathbf{G}-\mathbf{G}'}, \quad (33)$$

$$B_{\mathbf{G}-\mathbf{G}'} = \alpha_{\mathbf{G}-\mathbf{G}'}(G_x + G_x'), \quad (34)$$

and

$$C_{\mathbf{G}-\mathbf{G}'} = \alpha_{\mathbf{G}-\mathbf{G}'}\mathbf{G}\cdot\mathbf{G}' + i\omega\beta_{\mathbf{G}-\mathbf{G}'}. \quad (35)$$

The Eq. (32) defines a set of equations that give a matrix equation in the form

$$(k_x^2\mathbf{A} + k_x\mathbf{B} + \mathbf{C})\mathbf{T} = 0. \quad (36)$$

Here **A**, **B** and **C** are matrices with $n\times n$ elements given by $A_{\mathbf{G}-\mathbf{G}'}$,$B_{\mathbf{G}-\mathbf{G}'}$ and $C_{\mathbf{G}-\mathbf{G}'}$ defined by Eqs. (33)-(35) .

We reformulate the Eq. (36) as a complex eigenvalue problem in the form

$$\begin{pmatrix}\mathbf{C} & \mathbf{B}\\ \mathbf{O} & \mathbf{I}\end{pmatrix}\begin{bmatrix}\mathbf{T}\\ k_x\mathbf{T}\end{bmatrix} = k_x\begin{pmatrix}\mathbf{O} & -\mathbf{A}\\ \mathbf{I} & \mathbf{O}\end{pmatrix}\begin{bmatrix}\mathbf{T}\\ k_x\mathbf{T}\end{bmatrix}, \quad (37)$$

where $\mathbf{I}$ and $\mathbf{O}$ are matrices of size $n\times n$ that define the identity-matrix and the zero-matrix, respectively. From Eq. (37) we may obtain a complex wave vector k_x corresponding to the $\mathbf{\Gamma}\rightarrow\mathbf{X}$ direction for a given real frequency ω. By performing a frequency scan, we can obtain the complex band structure.

3.2. $\mathbf{\Gamma}\rightarrow\mathbf{M}$ direction

In this case, the wave vector is in the $\mathbf{\Gamma}\rightarrow\mathbf{M}$ direction. The wave vector is $\mathbf{k} = (k_x, k_y)$, but in this case the k_y component is equal to k_x, $k_y = k_x$. For this direction, we proceed similarly to the previous direction $\mathbf{\Gamma}\rightarrow\mathbf{X}$. Starting with Eq. (31) we obtain a set of equations that can be written in the same manner as Eq. (32). The difference is that in this case, the matrix elements are defined by the relations

$$A_{\mathbf{G}-\mathbf{G}'} = \alpha_{\mathbf{G}-\mathbf{G}'}, \quad (38)$$

$$B_{\mathbf{G}-\mathbf{G}'} = \frac{1}{2}\alpha_{\mathbf{G}-\mathbf{G}'}(G_x + G_x' + G_y + G_y'), \quad (39)$$

and

$$C_{\mathbf{G}-\mathbf{G}'} = \frac{1}{2}\alpha_{\mathbf{G}-\mathbf{G}'}\mathbf{G}\cdot\mathbf{G}' + \frac{1}{2}i\omega\beta_{\mathbf{G}-\mathbf{G}'}. \quad (40)$$

3.3. $\mathbf{X}\rightarrow\mathbf{M}$ direction

In this case, the wave vector is $\mathbf{k} = (\pi/D, k_y)$. Starting with Eq. (31) we obtain an eigenvalue equation for k_y in the form

$$(k_y^2\mathbf{A} + k_y\mathbf{B} + \mathbf{C})\mathbf{T} = 0, \quad (41)$$

where the elements of the matrices **A**, **B** and **C** are given by

$$A_{\mathbf{G}-\mathbf{G}'} = \alpha_{\mathbf{G}-\mathbf{G}'}, \quad (42)$$

$$B_{\mathbf{G}-\mathbf{G}'} = \frac{1}{2}\alpha_{\mathbf{G}-\mathbf{G}'}(G_y + G_y'), \quad (43)$$

and

$$C_{\mathbf{G}-\mathbf{G}'} = \alpha_{\mathbf{G}-\mathbf{G}'}\left[\mathbf{G}\cdot\mathbf{G}' + \frac{\pi}{d}(G_x + G_x' + \left(\frac{\pi}{d}\right)^2\right] + i\omega\beta_{\mathbf{G}-\mathbf{G}'}. \quad (44)$$

The Eq. (41) can be written as an eigenvalue problem as the form

$$\begin{pmatrix} \mathbf{C} & \mathbf{B} \\ \mathbf{O} & \mathbf{I} \end{pmatrix} \begin{bmatrix} \mathbf{T} \\ k_y \mathbf{T} \end{bmatrix} = k_y \begin{pmatrix} \mathbf{O} & -\mathbf{A} \\ \mathbf{I} & \mathbf{O} \end{pmatrix} \begin{bmatrix} \mathbf{T} \\ k_y \mathbf{T} \end{bmatrix}, \qquad (45)$$

where k_y is the complex eigenvalue.

4. Numerical results

We now apply the theory described in Section II to the case of a 2D square array of rectangular bars. The material a is a stratum-like material, and the layer b is a dermis-like material [11]. For the material a we have the following parameters: thermal conductivity $k_a = 0.235$ W m^{-1} K^{-1}, specific heat $c_a = 3600$ J kg^{-1} K^{-1}, density $\rho_a = 1500$ kg m^{-3}, and time delay $\tau_a = 1$ s. For the material b we have the following parameters: thermal conductivity $k_b = 0.445$ W m^{-1} K^{-1}, specific heat $c_b = 3300$ J kg^{-1} K^{-1}, density $\rho_b = 1116$ kg m^{-3}, and relaxation time $\tau_b = 20$ s. The period of the unit cell is $D = 0.001$ m.

As a specific application of our method, we consider the case of a filling fraction $f = 0.7$ For the calculation of the band structure shown here we use a total of 121 plane waves. However, the calculation was also performed with 196 plane waves and no difference was observed in the band structure. The band structure is shown in Fig. 2, where the wave vectors are in the abscissa coordinate, and in the ordinate coordinate we have the frequency, $\nu = \omega/(2\pi)$. The main effect of this band structure is the existence of a complete band gap through the whole First Brillouin Zone, which is illustrated in red color. We also observed a line in the $\mathbf{M\Gamma}$ that we mark with a green arrow. These solutions correspond to evanescent modes and have been previously reported in PCs where the PWM has been applied to calculate the complex relation dispersion. [13,14,32].

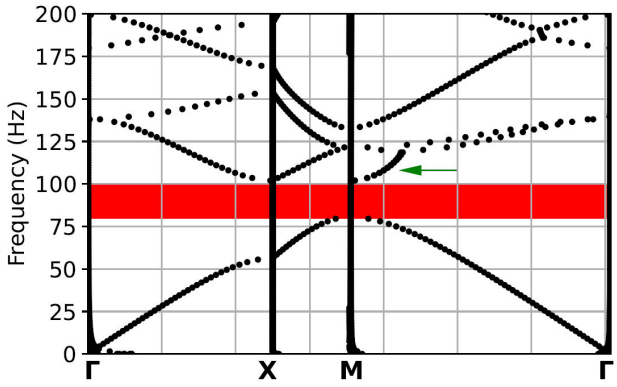

FIGURE 2. Band structure for thermal waves of a 2D TWC composed of an arrangement of square bars in a square lattice. The bars are made of materials a and the surrounding background has material b. The filling fraction of material a in the unit cell is $f = 0.7$. We observe a complete band gap with red color.

5. Conclusions

For computing the band structure of thermal waves, we have developed a theoretical formalism. We found that an eigenvalue problem for the frequency cannot be obtained for the CV model. The wave vector at a certain frequency may nevertheless be determined by solving an eigenvalue problem. We applied our formalism to the calculation of a square array of square bars of stratum-like material in a dermis-like material background. We achieve a well-converged band structure, in which exists a complete band gap in the FBZ.

1. H. D.Weymann, Finite speed of propagation in heat conduction, diffusion, and viscous shear motion, American *Journal of Physics* **35** (1967) 488. https://doi.org/10.1119/1.1974155
2. M. Chester, Second sound in solids, *Physical Review* **131** (1963) 2013. https://doi.org/10.1103/physrev.131.2013
3. D. D. Joseph and L. Preziosi, Heat waves, *Reviews of Modern Physics* **61** (1989) 41. https://doi.org/10.1103/revmodphys.61.41
4. M. Wang, N. Yang, and Z.-Y. Guo, Non-fourier heat conductions in nanomaterials, *Journal of Applied Physics* **110** (2011) 064310. https://doi.org/10.1063/1.3634078
5. A. I. Zhmakin, Non-Fourier Heat Conduction (Springer International Publishing, 2023). https://doi.org/10.1007/978-3-031-25973-9
6. C. Cattaneo, A form of heat-conduction equations which eliminates the paradox of instantaneous propagation, *Comptes Rendus* **247** (1958) 431.
7. P. Vernotte, Les paradoxes de la theorie continue de l'equation de la chaleur, *Comptes rendus* **246** (1958) 3154.
8. D. S. Chandrasekharaiah, Hyperbolic thermoelasticity: A review of recent literature, *Applied Mechanics Reviews* **51** (1998) 705. https://doi.org/10.1115/1.3098984
9. D. Y. Tzou, The generalized lagging response in smallscale and high-rate heating, *International Journal of Heat and Mass Transfer* **38** (1995) 3231. https://doi.org/10.1016/0017-9310(95)00052-b
10. S. K. R. Choudhuri, On a thermoelastic three-phase-lag model, *Journal of Thermal Stresses* **30** (2007) 231. https://doi.org/10.1080/01495730601130919
11. A.-L. Chen, Z.-Y. Li, T.-X. Ma, X.-S. Li, and Y.-S.Wang, Heat reduction by thermal wave crystals, International *Journal of Heat and Mass Transfer* **121** (2018) 215. https://doi.org/10.1016/j.ijheatmasstransfer.2017.12.136
12. R. D. V. Meade, S. G. Johnson, and J. N. Winn, Photonic crystals: *Molding the flow of light* (2008).

13. E. Guevara-Cabrera, M. Palomino-Ovando, B. Flores- Desirena, and J. Gaspar-Armenta, Dispersive photonic crystals from the plane wave method, *Physica B: Condensed Matter* **484** (2016) 53. https://doi.org/10.1016/j.physb.2015.12.030

14. S. Brand, R. Abram, and M. Kaliteevski, Complex photonic band structure and effective plasma frequency of a two-dimensional array of metal rods, *Physical Review B* **75** (2007) 035102. https://doi.org/10.1103/PhysRevB.75.035102

15. M. Maldovan, Narrow low-frequency spectrum and heat management by thermocrystals, *Physical Review Letters* **110** (2013) 025902. https://doi.org/10.1103/physrevlett.110.025902

16. L. Xu, J. Huang, and X. Ouyang, Tunable thermal wave nonreciprocity by spatiotemporal modulation, *Phys. Rev. E* **103** (2021) 032128. https://doi.org/10.1103/PhysRevE.103.032128

17. Z. Zhang, L. Xu, X. Ouyang, and J. Huang, Guiding temperature waves with graded metamaterials, Thermal Science and Engineering Progress **23** (2021) 100926. https://doi.org/10.1016/j.tsep.2021.100926

18. A. Camacho de la Rosa, D. Becerril, M. G. Gómez- Farfán, and R. Esquivel-Sirvent, Bragg mirrors for thermal waves, *Energies* **14** (2021). https://doi.org/10.3390/en14227452

19. G. Morales-Morales and J. Manzanares-Martinez, Enlargement of band gaps on thermal wave crystals by using heterostructures, *Results in Physics* **42** (2022) 106019. https://doi.org/10.1016/j.rinp.2022.106019

20. K. Xu and C. Jiang, Expanding the bandgap of thermal phonons by using supercrystals, *Results in Physics* **17** (2020) 103015. https://doi.org/10.1016/j.rinp.2020.103015

21. J. Ordonez-Miranda, Y. Guo, J. J. Alvarado-Gil, S. Volz, and M. Nomura, Thermal-wave diode, *Phys. Rev. Appl.* **16** (2021) L041002. https://doi.org/10.1103/PhysRevApplied.16.L041002

22. J. Wang, G. Dai, and J. Huang, Thermal metamaterial: Fundamental, application, and outlook, *iScience* **23** (2020) 101637. https://doi.org/10.1016/j.isci.2020.101637

23. T.-Z. Yang, Y. Su, W. Xu, and X.-D. Yang, Transient thermal camouflage and heat signature control, *Applied Physics Letters* **109** (2016). https://doi.org/10.1063/1.4963095

24. A. A. Zul Karnain, S. A. R. Kuchibhatla, T. Thomas, and P. Rajagopal, Semiconductor-based thermal wave crystals, *ISSS Journal of Micro and Smart Systems* **9** (2020) 181. https://doi.org/10.1007/s41683-020-00061-2

25. A. Camacho de la Rosa, D. Becerril, M. G. Gómez- Farfán, and R. Esquivel-Sirvent, Bragg mirrors for thermal waves, *Energies* **14** (2021) 7452. https://doi.org/10.3390/en14227452

26. G. Morales-Morales and J. Manzanares-Martinez, Enlargement of band gaps on thermal wave crystals by using heterostructures, *Results in Physics* **42** (2022) 106019. https://doi.org/10.1016/j.rinp.2022.106019

27. Z.-Y. Li, T.-X. Ma, A.-L. Chen, Y.-S. Wang, and C. Zhang, Thermal wave crystals based on the dualphase- lag model, *Results in Physics* **19** (2020) 103371. https://doi.org/10.1016/j.rinp.2020.103371

28. C. A. Romero-Ramos, B. Manzanares-Martinez, D. Soto-Puebla, and J. Manzanares-Martinez, Complex band structure of thermal wave crystals: The plane-wave method, *Rev. Mex. Fis.* **70** (2024) 031601. https://doi.org/10.31349/RevMexFis.70.031601

29. R. Shirzadkhani, S. Eskandari, and A. Akbarzadeh, Non-fourier thermal wave in 2d cellular metamaterials: From transient heat propagation to harmonic band gaps, *International Journal of Heat and Mass Transfer* **205** (2023) 123917. https://doi.org/10.1016/j.ijheatmasstransfer.2023.123917

30. Z.-Y. Li *et al.* Non-fourier heat conduction in 2d thermal metamaterials, *Materials Today Communications* **38** (2024) 107828. https://doi.org/10.1016/j.mtcomm.2023.107828

31. J. D. Jackson, Classical electrodynamics (1999).

32. M. Botey *et al*., Unlocked evanescent waves in periodic structures, *Optics Letters* **38** (2013) 1890. https://doi.org/10.1364/OL.38.001890